



ACADEMIC
PRESS

Available online at www.sciencedirect.com

SCIENCE @ DIRECT®

Journal of Magnetic Resonance 164 (2003) 44–53

JMR
Journal of
Magnetic Resonance

www.elsevier.com/locate/jmr

Comparison of electron spin relaxation times measured by Carr–Purcell–Meiboom–Gill and two-pulse spin-echo sequences

James R. Harbridge, Sandra S. Eaton, and Gareth R. Eaton*

Department of Chemistry and Biochemistry, University of Denver, Denver, CO 80208-2436, USA

Received 20 January 2003; revised 16 May 2003

Abstract

Electron spin relaxation times obtained by two-pulse spin-echo and Carr–Purcell–Meiboom–Gill (CPMG) experiments were compared for samples with: (i) low concentrations of nuclear spins, (ii) higher concentrations of nuclear spins and low concentrations of unpaired electrons, (iii) higher concentrations of nuclear spins and of electron spins, and (iv) dynamic averaging of inequivalent hyperfine couplings on the EPR timescale. In each case, the CPMG time constant decreased as the time between the refocusing pulses increased. For the samples with low concentrations of nuclear spins (the E' center in irradiated amorphous SiO_2) the limiting value of the CPMG time constant at short interpulse spacings was similar to the T_m obtained by two-pulse spin echo at small turning angle. For the other samples, the time constants obtained by CPMG at short interpulse spacings were systematically longer than T_m obtained by two-pulse spin echo. For most of the samples, the CPMG time constant decreased with increasing electron spin concentration, which is consistent with the expectation that the CPMG sequence does not refocus dephasing due to electron–electron dipolar interaction between resonant spins. Dynamic processes that average inequivalent hyperfine couplings contributed less to the CPMG time constant than to the spin-echo decay time constant. The impact of nuclear echo envelope modulation on CPMG time constants also was examined. For a Nycomed trityl radical in glassy D_2O :glycerol- d_8 solution, the CPMG time constant was up to 20 times longer when the time between pulses was approximately equal to integer multiples of the reciprocal of the deuterium Larmor frequency than when the time between pulses was an odd multiple of half the reciprocal of the deuterium Larmor frequency.

© 2003 Elsevier Science (USA). All rights reserved.

1. Introduction

The Carr–Purcell–Meiboom–Gill (CPMG) pulse sequence ($90_x^\circ - (\tau - 180_y^\circ - \tau)_n$ -echo, Fig. 1b) has been widely used in NMR [1–8], but there have been only a few reports of its applications in EPR [9–14]. This pulse sequence refocuses the contributions from time-independent processes that are described in the spin Hamiltonian by terms that are linear in electron spin, including magnetic field inhomogeneity and heteronuclear interactions [4]. Dipolar interaction between a resonant electron spin and a non-resonant electron spin is analogous to a heteronuclear interaction and is refocused [4]. Although the CPMG pulse sequence does not refocus the effects of time-dependent processes that occur on the timescale of the experiment, the impact of

these processes can be minimized if the time between refocusing pulses, 2τ , is short compared with the time constant for the process. The CPMG sequence does not refocus the contributions from processes that are described in the Hamiltonian by terms that are quadratic in electron spin. These quadratic terms include dipolar interaction between resonant spins [4], so CPMG is a powerful NMR technique for examining homonuclear dipolar coupling [5,6], even in solids. Heteronuclear NMR CPMG spin relaxation methods are important tools in characterizing dynamic processes in proteins [7]. In an ideal CPMG experiment, pulses are exactly $\pi/2$ or π . However, in most experiments B_1 is not large enough to excite all of the spins in broad EPR spectra. Spins that are slightly off resonance, but still excited, are turned by smaller angles than the spins that are exactly on resonance, which contributes to enhanced CPMG dephasing rates [12]. Enhanced rates of dephasing also are encountered when NMR CPMG experiments are

* Corresponding author. Fax: 1-303-871-2254.

E-mail address: geaton@du.edu (G.R. Eaton).

performed in solids or inhomogeneous magnetic fields [15].

Although contributions to two-pulse electron spin-echo decays from instantaneous diffusion, nuclear spin diffusion, and dynamic processes have been characterized in a few cases [16–21], the contributions of these processes to EPR CPMG decay curves have not been described previously. In this report we compare two-pulse spin-echo and CPMG time constants for samples for which spin–lattice relaxation and spin diffusion processes have been characterized previously by long-pulse saturation recovery, inversion recovery, and pulsed ELDOR [22,23]. The samples have a substantial range of nuclear spin concentrations and electron spin concentrations and some have dynamic processes that are occurring on the EPR timescale. Two-pulse spin-echo and CPMG time constants also are compared for a sample with deuterium echo envelope modulation.

Instantaneous diffusion occurs when the spin flips caused by the 90° pulse change the magnetic field at a neighboring spin enough to remove an excited spin from the set of spins that can be refocused by the 180° pulse [24,25]. Instantaneous diffusion tends to dominate electron spin-echo dephasing when other contributions are small, such as when nuclear spin concentrations are low, and when there are no thermally activated processes occurring at rates comparable to inequivalent hyperfine interactions. The effects of instantaneous diffusion can be decreased by (a) reducing the radical concentration, (b) changing the field (frequency) position of the excitation pulse so that fewer spins are excited, and (c) decreasing the pulse turning angle by reducing the pulse length or reducing B_1 [24,25].

A flip of a nuclear spin in the vicinity of the unpaired electron changes the local magnetic field at the electron, which changes the precessional frequency. Increasing frequency of nuclear spin flips causes faster echo dephasing and shorter T_m . The importance of nuclear spin diffusion in NMR [26–28] and EPR [16–18,29] has been described. Nuclear spin diffusion dominates electron spin phase memory times when the concentration of nuclear spins in the environment of the unpaired electron is high [17,30–32] and/or other contributions are small. Nuclear spin diffusion is an important relaxation process for radicals in irradiated organic solids, because there are many protons in the environment of the unpaired electron.

Spin-echo, continuous wave (CW), and electron-nuclear double resonance (ENDOR) measurements are sensitive to molecular motions occurring at a rate comparable to the inequivalences in hyperfine splittings that are averaged by the motion [19–21,29,33–36]. CW and ENDOR line shapes change if the couplings that are averaged by the rotation are significant relative to the linewidths. Spin-echo measurements can detect processes that average inequivalent couplings that are too

small to detect by CW-EPR. For radicals that contain a strongly coupled methyl group that is rotating at a frequency comparable to inequivalences in hyperfine splittings, T_m may become so short that a spin echo is not observed. Thermally activated processes generate a distinctive temperature dependence of T_m in the temperature range in which the rate is comparable to inequivalences that are averaged by the motion, so these processes are readily distinguished from other relaxation processes [16,19–21].

2. Experimental

2.1. Samples

Polycrystalline organic solids were irradiated at room temperature (20°C) with ^{60}Co γ -radiation to a dose of approximately 2.3, 6, or 20 mrad. Several types of vitreous SiO_2 (approximately 2 mm o.d. by 10 mm long cylinders) were irradiated to about 5.8 or 24 mrad with ^{60}Co γ -rays. One SiO_2 sample was irradiated with residual radiation from a nuclear reactor, with a dose that was calibrated to be equivalent to a ^{60}Co dose of about 0.9 mrad. After irradiation, samples were stored in air at room temperature. Local spin concentrations for the SiO_2 samples were determined by instantaneous diffusion [25,37]. Spin concentrations for the organic solids were determined by comparison of double-integrated first-derivative CW spectra with spectra for a 0.53 mM solution of 2,2,6,6-tetramethyl-piperidinyloxy (Aldrich Chemical, Milwaukee, WI) in toluene. For these polycrystalline samples, spin concentrations were calculated as spins/cm³, where the volume refers to the loosely packed irregular solid. The packing efficiency for the irradiated solids is about 0.6 cm³ of solid per 1 cm³ of space in the EPR tube [22], so spin concentrations per cm³ of solid are about 1.6 times higher than the values calculated by comparison with the fluid solution standard. Except for the plot in Fig. 8, spin concentrations in this report are given per cm³ of space in the EPR tube. Experiments were performed weeks to months, or longer, after irradiation, and no significant radical degradation as a function of time was observed.

2.2. Spectroscopy

The spin-echo and CPMG pulse sequences are shown in Fig. 1. Data were acquired at X-band on a locally built spectrometer equipped with a 20 W continuous wave TWT, a modified Varian TE₁₀₂ cavity resonator, and a quartz dewar insert [38]. The resonator was over-coupled to $Q \sim 120$ –150. The length of a 90° pulse range ranged from 50 to 65 ns, depending on the degree of resonator over-coupling. In the system that was used

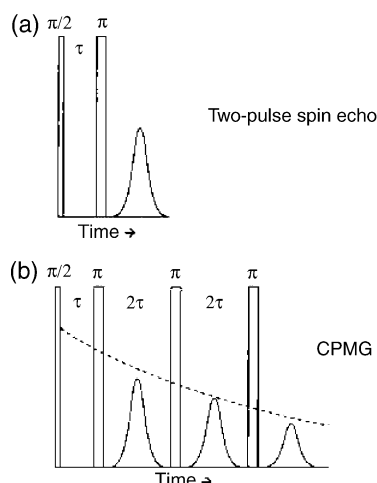


Fig. 1. (a) Two-pulse spin-echo sequence. (b) Carr–Purcell–Meiboom–Gill (CPMG) pulse sequence. The figure was adapted from [56].

for these experiments τ could be stepped in increments of 1 ns, which permitted measurement of T_m values as short as about 100 ns. The hardware/software for these experiments was limited to 256 CPMG refocusing pulses, with a minimum time between pulses of 64 ns, which restricted the CPMG measurements to time constants longer than about 600 ns. For variable temperature experiments the samples were cooled by nitrogen gas flowing through a coil immersed in liquid nitrogen. A single exponential was fitted to each decay curve using a Levenberg–Marquardt algorithm. For the CPMG experiments with short interpulse spacings, and for electron spin decays without echo modulation, a single exponential gave a good fit to the data, and the uncertainty in the time constants was about 10%. As the interpulse spacings were increased, or for samples that exhibit electron spin-echo modulation, a single exponential did not fit well to some of the decays, so the parameters from the single exponential fits were used primarily for comparison of experiments. The following notation is used: T_m is the spin-echo dephasing time constant and T_2 is the contribution to dephasing from electron–electron dipolar interaction.

3. Results

3.1. Samples with few nuclear spins

In vitreous SiO_2 there are few nuclear spins (^{29}Si is 4.7% abundant) and spin-echo decays for the E' center in irradiated SiO_2 are strongly impacted by instantaneous diffusion [25]. Spin-echo and CPMG experiments were performed for the E' centers in six irradiated SiO_2 samples with local spin concentrations ranging from 1.2×10^{16} to 4.9×10^{17} spins/cm³ (Table 1). The differences in spin concentrations for different samples irradiated to the same dose reflect the dependence of radical formation on the characteristics of the SiO_2 [39,40]. Spin-echo values of T_m were determined by extrapolation of $1/T_m$ to small turning angle [25]. For each of the samples, as the time between refocusing pulses was increased, the CPMG decay time constant decreased (Fig. 2). Some of the dependence on interpulse spacing is attributed to effective turning angles less than 180° for spins that are slightly off-resonance. The dependence of the CPMG time constant on interpulse spacing increased as the spin concentration increased, which is attributed to a contribution from electron–electron dipolar coupling that is not refocused by the CPMG experiment [4]. Extrapolation to negligible time between refocusing pulses gave CPMG time constants that are within a factor of 2 of the spin-echo time constants at small turning angle [37]. The shorter values of T_m than of the CPMG decay constants, particularly for the samples with the longest values of T_m (Table 1), may reflect the difficulty of mitigating the effects of instantaneous diffusion on the spin-echo decays. For sample #1 the room temperature value of T_m is impacted by T_1 , which is 200 μs [37]. When sample #1 was cooled to 77 K, T_1 was much longer than T_m , and a CPMG time constant of 830 μs was obtained. Except when driven by T_1 or in temperature intervals where a thermally activated process averages inequivalent nuclear environments on the EPR timescale, T_m is independent of temperature [16–18], so the low-temperature value of T_m for sample #1 is used in the ensuing comparisons of the values for the irradiated SiO_2 samples. As discussed

Table 1
Irradiated vitreous SiO_2 samples

Sample	Radiation dose (mrad)	Local spin concentration ^a (spins/cm ³)	T_m ^b (ESE) (μs), at 20 °C	CPMG time constant (μs), at 20 °C
1	0.9	1.2×10^{16}	120 ^c	200
2	5.8	1.3×10^{17}	58	110
3	24	2.4×10^{17}	44	55
4	5.8	2.9×10^{17}	40	50
5	24	3.6×10^{17}	35	40
6	24	4.9×10^{17}	31	30

^a Local spin concentration calculated from instantaneous diffusion, measured by the dependence of T_m on pulse turning angle [37].

^b Value of T_m measured by two-pulse spin echo, extrapolated to small turning angle.

^c Value at 77 K is 830 μs .

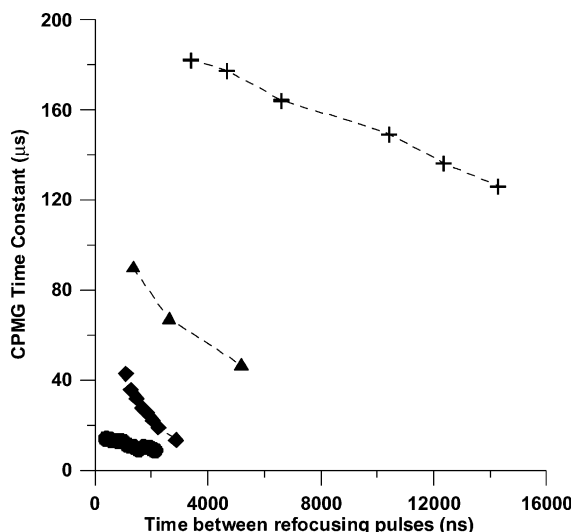


Fig. 2. Room temperature CPMG time constants as a function of the time between the refocusing pulses: (+) Irradiated SiO₂ sample 1, (▲) irradiated SiO₂ sample 2, (◆) irradiated SiO₂ sample 3, and (●) irradiated malonic acid [2.3 mrad dose, 8.8×10^{17} spins/cm³]. The lines connect the data points.

below, T_m and the CPMG time constants for the irradiated SiO₂ samples decreased as the spin concentration increased (Table 1), consistent with domination of the dephasing by dipolar interaction between the unpaired electrons.

The dephasing time constants for the E' signals show that for samples with low nuclear spin concentration and negligible effects from thermally activated processes, the electron–electron dipolar T_2 can be obtained by either two-pulse spin echo at small turning angle or by CPMG with short interpulse spacings. In the following paragraphs, data are discussed for samples with substantial nuclear spin concentrations and/or thermally activated processes. To minimize the effects of instantaneous diffusion on these comparisons, two-pulse spin-echo data were obtained with small turning angles. CPMG time constants were measured with times between the re-focusing pulses of 340–540 ns. Shorter interpulse spacings were used for the samples with shorter two-pulse echo decay times.

3.2. Samples with higher concentrations of nuclear spins

Values of the decay constants obtained by spin echo or CPMG for samples of malonic acid (Table 2) irradiated at about 2.3 mrad (8.8×10^{17} spins/cm³) or 24 mrad (2.7×10^{18} spins/cm³) were indistinguishable, within experimental uncertainty, and were independent of temperature between about 77 and 160 K (Fig. 3), which is consistent with domination of the echo dephasing by proton spin diffusion [16–18], and not electron–electron dipolar interaction. The CPMG time constant decreased with increasing interpulse spacing (Fig. 2), which is attributed to turning angles less than

180° for some off-resonance spins. The comparisons in Fig. 3 are based on values obtained at short interpulse spacings. The longer time constants obtained by CPMG than by two-pulse spin echo indicate that the CPMG decays have a smaller contribution from nuclear spin diffusion than do the spin-echo decays (see Table 2).

3.3. Samples with higher nuclear spin and electron spin concentrations

Values of the spin-echo and CPMG time constants for irradiated glycylglycine (Table 2) were substantially longer for a sample irradiated at a dose of 2.3 mrad (3.6×10^{18} spins/cm³) than for a sample irradiated at 24 mrad (2.1×10^{19} spins/cm³) (Fig. 3), which indicates that electron–electron dipolar interaction made a substantial contribution to echo dephasing at these radical concentrations. For both doses, the CPMG time constants were longer than T_m , which indicates that the CPMG sequence decreased the impact of processes that made substantial contributions to the spin-echo time constants.

3.4. Samples with thermally activated processes that average inequivalent hyperfine interactions

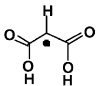
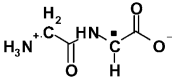
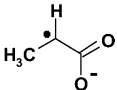
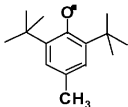
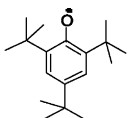
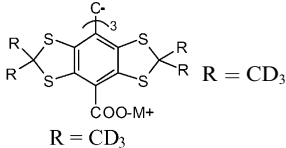
In temperature intervals where the rate of a process is comparable to the inequivalence in the hyperfine couplings that are averaged, the CW spectrum is broadened and T_m is decreased [41]. Since these processes can cause T_m to become very short, it is of particular interest to see how these processes impact the CPMG decays.

Above about 160 K, the time constants obtained by two-pulse spin echo or CPMG for irradiated malonic acid and glycylglycine decreased (Fig. 3), which is attributed to physical motions that average protons with inequivalent couplings to the unpaired electron. For glycylglycine the effects of the dynamic process, which is easily observed for the sample with low electron spin concentration, are masked by the strong electron–electron dipole interactions in the sample with the highest electron spin concentration studied (Fig. 3). These radicals do not contain methyl groups, so it is proposed that the process that affects the dephasing for both radicals above 160 K involves hydrogen bonding [23]. Above 160 K, the time constants observed in the CPMG experiments were longer than in the two-pulse spin-echo experiments, which suggest that the refocusing pulses eliminate some of the effects of the thermally activated process.

3.4.1. Effect of methyl rotation on dephasing for irradiated L-alanine

For the radical in irradiated L-alanine (Table 2) the barrier to rotation of the strongly coupled α -methyl

Table 2
EPR parameters for samples studied

Radical	Host	Spectral parameters at room temperature ^a	Prior information concerning spin system
E' center	Vitreous SiO ₂	g Anisotropy gives spectral extent of about 4 G at X-band	Most of spectrum excited by B_1
	Malonic acid	Two resolved hyperfine bands, $A_H \sim 23$ G, l.w. ~ 8 G	Spectral diffusion makes little contribution to inversion recovery measurements at 20 °C [23]
	Glycylglycine	Two resolved hyperfine bands, $A_H \sim 19$ G, l.w. ~ 15 G	Rapid spectral diffusion within and between the hyperfine lines at 20 °C [22]
	L-alanine	Five resolved hyperfine bands, $A_H \sim 25$ G, l.w. ~ 12 G	Rotation of methyl group is fast on EPR timescale and there is rapid cross-relaxation at 20 °C [22]
	4-methyl-2,6- <i>t</i> -butyl phenol	Four resolved hyperfine bands, $A_H \sim 11$ G, l.w. ~ 11 G	Rotation of 4-methyl group is much faster than 9 GHz at 20 °C. Spectral diffusion makes little contribution to inversion recovery curves at RT [22]
	2,4,6-tri- <i>t</i> -butyl phenol	Hyperfine splitting is unresolved, l.w. ~ 14 G	Spectral diffusion makes negligible contribution to inversion recovery curves at 20 °C [22]
	Water	Single inhomogeneously broadened line with l.w. ~ 48 mG	There is echo envelope modulation from the CD ₃ deuterons at 77 and 90 K

^a Linewidths are full-width at half maximum.

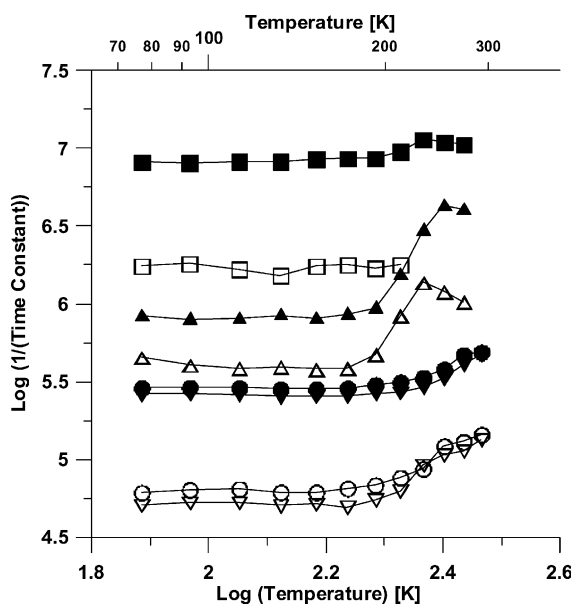


Fig. 3. Temperature dependence of $1/T_m$ for irradiated: (■) glycyglycine (24 mrad dose, 2.1×10^{19} spins/cm³), (▲) glycyglycine (2.3 mrad, 3.6×10^{18} spins/cm³), (●) malonic acid (24 mrad dose, 2.7×10^{18} spins/cm³), and (▼) malonic acid (2.3 mrad, 8.8×10^{17} spins/cm³). Temperature dependence of CPMG time constants for: (□) glycyglycine (24 mrad dose, 2.1×10^{19} spins/cm³), (△) glycyglycine (2.3 mrad, 3.6×10^{18} spins/cm³), (○) malonic acid (24 mrad dose, 2.7×10^{18} spins/cm³), and (▽) malonic acid (2.3 mrad, 8.8×10^{17} spins/cm³). The lines connect the data points.

group is about 15 kJ [42–45]. At constant inter-pulse spacing, the relative intensity of the echo decreases as T_m decreases. For the radical in irradiated L-alanine, field-swept echo-detected spectra at selected temperatures, obtained with $\tau = 192$ ns, are shown in Fig. 4. At 295 K, the ratios of the amplitudes of hyperfine lines in the echo-detected spectrum are about 1:4:5:4:1, which is close to the intensity ratios (1:4:6:4:1) that are observed in the CW absorption spectrum at 293 K [46]. The approach of the relative intensities in the echo-detected spectrum to those in the CW spectrum is consistent with the observation that T_m is similar for all of the transitions at room temperature.

As the temperature is decreased, the ratios of the amplitudes of the hyperfine lines in the echo-detected spectra change dramatically. Between 213 and 123 K the amplitude of the center-line is very small and the four other hyperfine lines have about equal amplitudes. The discrepancy at low temperature between the observed relative amplitudes and the approximately 1:4:5:4:1 ratio observed at higher temperatures indicates that between 213 and 123 K T_m is much shorter for some transitions than for others. The differences in the temperature dependence of the echo-detected intensities for the five hyperfine lines can be explained by the effects of methyl rotation. The rate of reorientation of the α -methyl group is slow relative to the inequivalences in the hyperfine couplings to the three methyl protons at 77 K

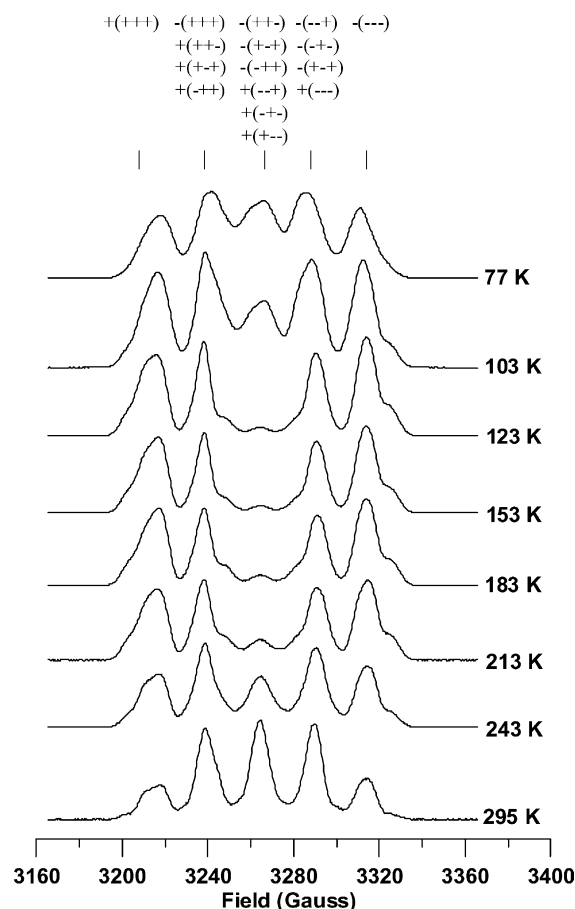


Fig. 4. X-band field-swept echo-detected spectra for L-alanine (5.7 mrad, 1.1×10^{19} spins/cm³) as a function of temperature. The time between pulses was 192 ns and the length of the 90° pulse was 30 ns. The spectra were scaled to approximately constant amplitude. The labeling at the top of the figure shows the combinations of the proton spin states, neglecting anisotropy, for the α -H and (in parentheses) for the three methyl protons that correspond to each of the five hyperfine lines.

and fast at 273 K. The anisotropy of the proton hyperfine couplings is relatively small, so the lines in the spectrum can be identified with combinations of proton spin states as shown in Fig. 4. The EPR transitions for the electron spin coupled to methyl proton spin states [(++-), (+-+), and (-++)] or [(--+), (-+-), and (+--)] are dependent on the methyl group rotation rate due to averaging of inequivalent environments. However, the transitions for the electron spin coupled to the (+++) and (---) methyl proton spin states are independent of the rate of rotation. Coupling to the α -proton splits each of the four lines from the methyl spin states into two [46]. The EPR lines with couplings to the [(++-), (+-+), and (-++)] or [(--+), (-+-), and (+--)] proton spin states have shorter T_m at temperatures where the methyl rotation frequency is comparable to inequivalences in the hyperfine couplings (between about 123 and 213 K) and therefore the relative intensities of these lines are

reduced in the echo-detected spectrum. The EPR lines with couplings to the (+++) and (---) proton spin states have longer T_m , and thus dominate the field-swept echo-detected spectra in the intermediate exchange region. The lines with couplings to proton spin state that are independent of methyl rotation rate contribute to the 5-line spectrum with intensities 1:1:0:1:1, as observed experimentally (Fig. 4). At low temperature, where the methyl protons are inequivalent on the EPR timescale, the couplings to the three protons are 5, 28, and 44 G [46]. Calculations based on the activation energy for rotation of the α -methyl group of the L-alanine radical [47] indicate that averaging of the large inequivalences in the hyperfine couplings would cause T_m to be less than 100 ns between about 110 and 210 K. This is approximately the temperature range in which the rotation-dependent lines make little contribution to the echo-detected spectra (Fig. 4).

Although T_m for the hyperfine lines that arise only from the (+++) or (---) spin states of the α -methyl protons (the highest- and lowest-field hyperfine lines in Fig. 4) are not impacted by α -methyl rotation, spin-echo and CPMG time constants for these lines are temperature dependent (Fig. 5, data shown only for the highest-field line). This temperature dependence is attributed to rotation of lattice methyl groups at rates comparable to the anisotropy in their small dipolar couplings to the unpaired electron. In the spin-echo data there are local maxima in $1/T_m$ at about 125 and 200 K (Fig. 5), which may be due to the effects of unique types of lattice methyls. These local maxima are less evident in the

CPMG data. The CPMG and spin-echo decay time constants for the sample with 20 mrad dose are shorter than for the sample with 5.7 mrad dose, which indicates that electron–electron dipolar interaction contributes more to the dephasing at the higher radiation dose (Fig. 5).

3.4.2. Effect of methyl rotation on dephasing for γ -irradiated 4-methyl 2,6-di-*t*-butyl phenol and 2,4,6-tri-*t*-butyl phenol

Fig. 6 shows the spin-echo and CPMG time constants for γ -irradiated 4-methyl 2,6-di-*t*-butyl phenol and 2,4,6-tri-*t*-butyl phenol (Table 2). In the temperature range examined, the 4-methyl group in the 4-methyl 2,6-di-*t*-butyl phenoxy radical rotates at a rate much faster than the inequivalences in the hyperfine splittings [48]. The temperature dependence of the spin-echo and CPMG rate constants between 77 and 295 K is attributed to *t*-butyl methyl groups rotating at rates comparable to inequivalences in their hyperfine splitting (\sim a few MHz). These couplings are too small to be resolved in the CW-EPR spectra. For the 4-methyl 2,6-di-*t*-butyl phenoxy radical, maxima in the dephasing rates were observed at two temperatures (\sim 110 and 220 K) suggesting that the *t*-butyl groups have distinctly different hyperfine couplings and/or the activation energies for individual methyl groups are different. NMR studies of unirradiated 4-methyl 2,6-di-*t*-butyl phenol found inequivalent rotation barriers for the methyls within the *t*-butyl groups [49,50]. For the 2,4,6 tri-*t*-butyl phenoxy

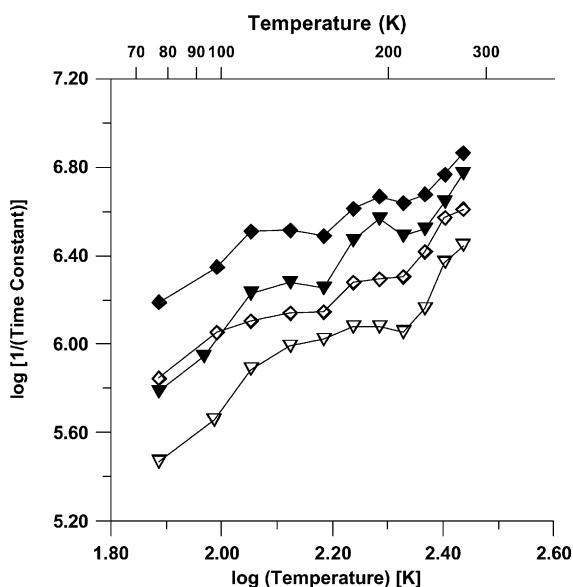


Fig. 5. Temperature dependence of time constants obtained for the highest-field hyperfine line in the spectrum of irradiated L-alanine for: (◆) two-pulse spin echo, 20 mrad dose; (▼) two-pulse spin echo, 5.7 mrad dose; (◇) CPMG, 20 mrad dose; and (▽) CPMG, 5.7 mrad dose. The lines connect the data points.

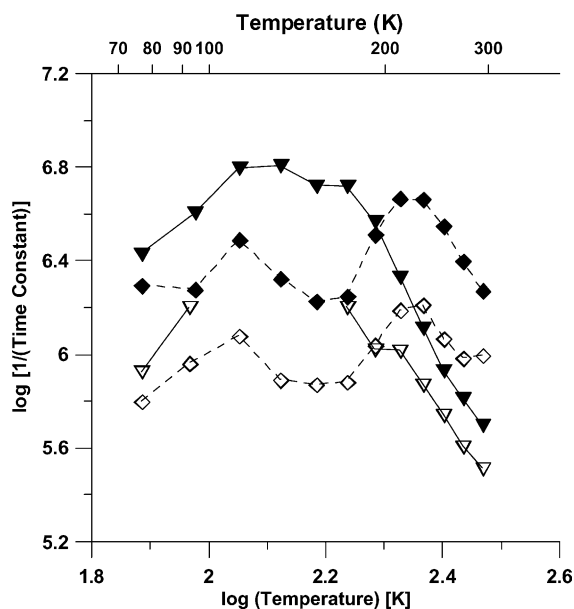


Fig. 6. Temperature dependence of time constants obtained for 4-methyl-2,6-di-*t*-butyl phenoxy radicals (2×10^{18} spins/cm³) by (◆) two-pulse spin echo or (◇) CPMG; and for 2,4,6-tri-*t*-butyl phenoxy radicals (3×10^{17} spins/cm³) by (▼) two-pulse spin echo or (▽) CPMG. The lines connect the data points.

radical the effects of methyl rotation are observed between 77 and 295 K with a maximum in the spin-echo rate at about 130 K (Fig. 6). CPMG time constants were not measured between 93 and 153 K because the decays were too fast to obtain enough CPMG data points to define a curve with our present hardware. The observation of a single broad maximum in $1/T_m$ indicates that the differences in barriers to rotation for different types of methyls are smaller for the 2,4,6 tri-*t*-butyl phenoxy radical than for the 4-methyl analog, which is consistent with previous studies [22].

For these two samples, in the temperature region examined, the similarity in the temperature dependence of T_m and the CPMG time constants indicate that the time constants from both experiments are dominated by methyl rotation.

3.5. Effects of electron spin-echo envelope modulation on CPMG decay curves

A distinctly different behavior of the CPMG time constant as a function of the time between refocusing pulses was observed for the Nycomed sym-trityl radical [51] (see Table 2) dissolved in deuterated solvents (Fig. 7). For this sample, the CPMG time constant varied sinusoidally with pulse timing. The time between the peaks in Fig. 7 is about 470 ns, which is equal to the reciprocal of the deuterium Larmor frequency at X-band. The times between the refocusing pulses for which the longest CPMG time constants were obtained correspond to peaks in the modulation of the spin-echo decay, while the shortest time constants correspond to

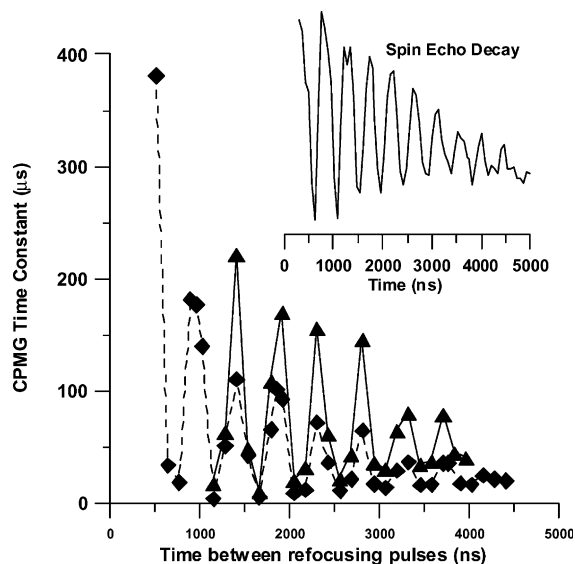


Fig. 7. CPMG time constants for 0.2 mM Nycomed trityl radical in 1:1 D_2O :glycerol- d_8 as a function of time between the refocusing pulses at (▲) 77 K and (◆) 99 K. A spin-echo decay curve at 40 K is displayed in the inset to show the echo envelope modulation that is observed for this sample. The lines connect the data points.

minima in the spin-echo decay (see Fig. 7, inset). The longest decay time, which presumably is the closest to the electron–electron dipolar T_2 , is obtained when the refocusing pulses occur at the maxima in the nuclear modulation cycles. When the timing of the CPMG refocusing pulses is synchronized with the modulation, the maximum magnetization is available for refocusing. At 99 K, the time constants at the local maxima for the data in Fig. 7 decreased from about 400 μs to about 40 μs as the spacing between pulses was increased from about 500 ns to about 3700 ns, which demonstrate the effects of other processes in addition to the nuclear modulation.

4. Discussion

4.1. What information can be obtained from CPMG or two-pulse spin-echo time constants?

For each of the irradiated solids studied, the CPMG time constant obtained with short interpulse spacing was longer than T_m , which indicates that the CPMG experiment decreases the contribution to dephasing from some processes. Since nuclear spin diffusion has greater impact on the spin-echo decays than on CPMG decays, spin echo is the preferred method for characterizing nuclear spin diffusion. Equations have been derived to relate the temperature dependence of T_m in a two-pulse experiment to the activation energy and magnitude of the inequivalence that is averaged [41]. Before a comparable analysis could be applied to CPMG data, it will be necessary to derive analogous expressions that account for the CPMG refocusing in partially excited spin systems.

In a CPMG experiment, when the time between pulses (t_{cp}) is much shorter than the dephasing time constant, a spin lock condition can be achieved and the CPMG time constant approaches $T_{1\rho}$ [52]. This condition also requires $t_{cp}\Delta \ll 1$, where Δ is the offset from resonance, which may be satisfied in some of the experiments reported here for the on-resonance spins and for some spins near resonance.

Bloch [53] proposed that the time constant for relaxation in the transverse plane, T_2 , could be estimated from the dipolar field as $T_2 \sim r^3/\gamma\mu$, where μ is the magnetic moment of the neighboring spins. Bloembergen et al. [54] cited this expression as

$$T_2 \sim \frac{\hbar r^3}{\mu^2} \quad (1)$$

making the substitution $\gamma = \mu/S\hbar$, but omitting the factor of S . When random occupancy of sites in the lattice is considered, the coefficients in Eq. (1) change, but a linear decrease of T_2 with increasing spin concentration is still expected [55–57]. The more difficult issue of how to account for the decreased probability of mutual spin flips due to differences in resonance

frequencies because of g and A anisotropy and dipolar interaction of the electron spin with nuclear spins has not been analyzed. In the present study we compare experimental values of decay time constants obtained by CPMG with the magnitude for T_2 predicted by Eq. (1). Comparison of experimental decay constants with the expected dependence of the dipolar interaction on spin concentration is an indication of the extent to which electron–electron dipolar interaction contributes to the observed time constants.

Fig. 8 shows the time constants obtained by CPMG in this study, plotted as a function of total electron spin concentration, for several different samples in temperature intervals in which the dephasing was not dominated by a thermally activated process. The solid line was calculated using Eq. (1) and agrees well with the experimental data for the E' centers in the irradiated SiO_2 samples, despite the fact that the expression was only an order of magnitude estimate [53]. Although the dipolar T_2 for the E' centers can also be obtained by two-pulse spin echo with extrapolation to small turning angle [37], the use of the CPMG sequence to measure decay times for samples such as irradiated SiO_2 , can save acquisition time relative to that which would be required in a spin-echo experiment to signal average the weaker signals at the very low powers required to extrapolate to small turning angles.

Although the values of the CPMG time constants for the irradiated solids generally follow the trend predicted based on electron–electron dipolar interactions (calculated using Eq. (1)), there are several confounding variables with respect to the experiment and to the pool

of spins that contribute to the dipolar T_2 . The spin concentrations that were used to calculate the line shown in Fig. 8 are the total spin concentration for each sample. For the E' centers in irradiated SiO_2 the microwave B_1 is large enough to excite the full spectrum, although the B_1 is not uniform over the full extent of the spectrum. For the broader spectra, B_1 excites only a fraction of the spins. For example, for the irradiated L-alanine sample the full spectral width is more than 100 G, so a B_1 of about 1.5 G excites a small fraction of the total spectrum. Dipolar coupling to off-resonance spins should be at least partially refocused by the CPMG sequence [3]. The differences in the resonance frequencies for various spins within the sample may limit the effective transfer of energy between spins that characterizes T_2 , which would decrease the effective spin concentration for the dipolar interaction. However a compensating factor is that efficient spectral diffusion processes may equilibrate magnetization with neighboring spin packets [22]. Thus it is difficult to estimate the fraction of the spins that contribute to the dipolar interaction that defines T_2 . Also, although the CPMG time constants for the irradiated malonic acid samples fall above the calculated line in Fig. 8 (longer time constant than predicted by the simple approximation of Eq. (1)), the weak dependence on spin concentration indicates that the dephasing is not dominated by electron–electron dipolar interaction. The observation of longer values of T_2 than predicted by the simple approximation may indicate that the effective spin concentration is lower than the bulk concentration because many of the spins in the broad spectrum are not on resonance.

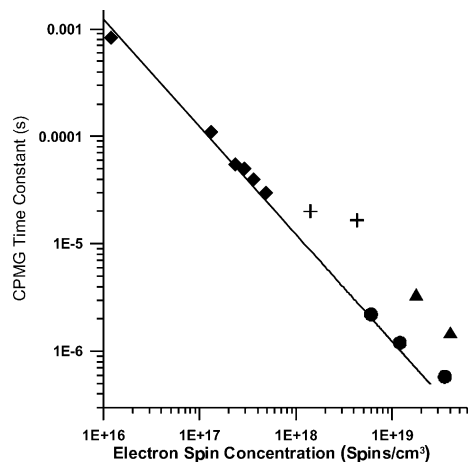


Fig. 8. CPMG time constants as a function of total electron spin concentration for: (◆) E' center in irradiated amorphous SiO_2 , (+) irradiated malonic acid, (●) irradiated glycylglycine, and (▲) irradiated L-alanine. Time constants were measured at temperatures where a thermally activated process does not contribute to dephasing. For the irradiated organic solids the spin concentrations per cm^3 volume in the EPR tube were multiplied by 1.6 as an approximate correction for the packing of the solid in the tube. The solid line was calculated using Eq. (1).

5. Conclusion

For samples with narrow EPR signals and few nuclear spins, T_2 due to electron–electron dipolar interaction could be determined either by two-pulse spin echo with extrapolation to small turning angle or by CPMG with short interpulse spacing. For irradiated organic solids the time constant obtained by CPMG tended to decrease with increasing spin concentration, as expected for electron–electron dipolar interaction. For radicals with broad spectra, differences in resonant frequencies may limit the number of spins that can exchange energy, so the effective spin concentration for dipolar interaction may be less than the total spin concentration.

The CPMG time constants that most closely approach the values determined by electron–electron dipolar interaction are obtained when the time between the refocusing pulses is as short as possible and when measurements are performed in a temperature range where dynamic processes do not contribute to the decay. Time-dependent processes contribute more to the

CPMG time constant as the time constant for the process becomes short relative to the time between refocusing pulses. These competing processes can be recognized by measuring CPMG time constants as a function of interpulse spacing and by measurements as a function of temperature. For radicals that exhibit electron spin-echo modulation, the spacing between refocusing pulses should be set to match the period of the modulation.

Acknowledgments

Support of this work by NIH Grant GM21156 is gratefully acknowledged. We thank Cobe Laboratories (Golden, CO) and Hugh Mallard (USGS) for irradiating the samples. Richard Quine wrote the software to implement the programmable timing unit for the pulse sequences used in these experiments.

References

- [1] H.Y. Carr, E.M. Purcell, *Phys. Rev.* 94 (1954) 630–638.
- [2] S. Meiboom, D. Gill, *Rev. Sci. Instrum.* 29 (1958) 688–691.
- [3] J.S. Waugh, C.H. Wang, *Phys. Rev.* 162 (1967) 209–216.
- [4] J.S. Waugh, C.H. Wang, L.M. Huber, R.L. Vold, *J. Chem. Phys.* 48 (1968) 662–670.
- [5] M. Engelsberg, *J. Magn. Reson.* 88 (1990) 393–400.
- [6] S.L. Grage, A.S. Ulrich, *J. Magn. Reson.* 138 (1999) 98–106.
- [7] A.G. Palmer III, C.D. Kroenke, J.P. Loria, *Methods Enzymol.* 339 (2001) 204–238.
- [8] M. Engelsberg, in: D.M. Grant, R.K. Harris (Eds.), *Encyclopedia of Nuclear Magnetic Resonance*, vol. 3, 1996, pp. 1696–1700.
- [9] C.E. Davoust, C.A. Hutchison, M.D. Kemple, H.-J. Kim, Y.-T. Yen, *Phys. Rev. B* 15 (1977) 5166–5180.
- [10] L.J. Schwartz, A.E. Stillman, J.H. Freed, *J. Chem. Phys.* 77 (1982) 5410–5424.
- [11] U. Eliav, J.H. Freed, *Rev. Sci. Instrum.* 54 (1983) 1416–1417.
- [12] V.V. Kurshev, A.M. Raitsimring, *J. Magn. Reson.* 88 (1990) 126–129.
- [13] P. Höfer, K. Holczer, D. Schmalbein, *Appl. Radiat. Isot.* 40 (1989) 1233–1235.
- [14] M. Brustolon, A.L. Maniero, M. Bonora, U. Segre, *Appl. Magn. Reson.* 11 (1996) 99–113.
- [15] F. Balibanu, K. Hailu, R. Eymael, D.E. Demco, B. Blümich, *J. Magn. Reson.* 145 (2000) 246–258.
- [16] S.S. Eaton, G.R. Eaton, in: *Biological Magnetic Resonance*, vol. 19, Kluwer Academic/Plenum Publishers, New York, 2000 (Chapter 2).
- [17] I.M. Brown, in: L. Kevan, R.N. Schwartz (Eds.), *Time Domain Electron Spin Resonance*, Wiley, New York, 1979, pp. 195–229.
- [18] M.K. Bowman, L. Kevan, in: L. Kevan, R.N. Schwartz (Eds.), *Time Domain Electron Spin Resonance*, Wiley, New York, 1979, pp. 68–105.
- [19] S.K. Hoffmann, J. Goslar, W. Hilczer, M.A. Augustyniak, M. Marciniak, *J. Phys. Chem. A* 102 (1998) 1697–1707.
- [20] S.K. Hoffmann, W. Hikczer, J. Goslar, S. Kiczka, I. Polus, *Phys. Chem. Chem. Phys.* 4 (2002) 4944–4951.
- [21] A. Barbon, M. Brustolon, A.L. Maniero, M. Romanelli, L.-C. Brunel, *Phys. Chem. Chem. Phys.* 1 (1999) 4015–4023.
- [22] J.R. Harbridge, S.S. Eaton, G.R. Eaton, *J. Phys. Chem.* 107 (2003) 598–610.
- [23] J.R. Harbridge, S.S. Eaton, G.R. Eaton, Electron spin relaxation of radicals in γ -irradiated malonic acid and methyl malonic acid, *Appl. Magn. Reson.*, in press.
- [24] J.R. Klauder, P.W. Anderson, *Phys. Rev.* 125 (1962) 912–932.
- [25] S.S. Eaton, G.R. Eaton, *J. Magn. Reson. A* 102 (1993) 354–356.
- [26] P.W. Anderson, *Phys. Rev.* 109 (1958) 1492–1505.
- [27] E.L. Wolf, *Phys. Rev.* 142 (1966) 555–569.
- [28] D. Tse, S.R. Hartmann, *Phys. Rev. Lett.* 21 (1968) 511–514.
- [29] A. Zecevic, G.R. Eaton, S.S. Eaton, M. Lindgren, *Mol. Phys.* 95 (1998) 1255–1263.
- [30] J.P. Gordon, K.D. Bowers, *Phys. Rev. Lett.* 1 (1958) 368–369.
- [31] I.M. Brown, *J. Chem. Phys.* 55 (1971) 2377–2384.
- [32] K.M. Salikhov, Yu.D. Tsvetkov, in: L. Kevan, R.N. Schwartz (Eds.), *Time Domain Electron Spin Resonance*, Wiley, New York, 1979, pp. 232–277.
- [33] K. Nakagawa, M.B. Candelaria, W.W. Chik, S.S. Eaton, G.R. Eaton, *J. Magn. Reson.* 98 (1992) 81–91.
- [34] J.-L. Du, G.R. Eaton, S.S. Eaton, *Appl. Magn. Reson.* 6 (1994) 373–378.
- [35] J.-L. Du, G.R. Eaton, S.S. Eaton, *J. Magn. Reson. A* 117 (1995) 67–72.
- [36] S. Saxena, J.H. Freed, *J. Chem. Phys. A* 101 (1997) 7998–8008.
- [37] J.R. Harbridge, G.A. Rinard, R.W. Quine, S.S. Eaton, G.R. Eaton, *J. Magn. Reson.* 156 (2002) 41–51.
- [38] R.W. Quine, G.R. Eaton, S.S. Eaton, *Rev. Sci. Instrum.* 63 (1992) 4251–4262.
- [39] M. Sueki, W.R. Austin, L. Zhang, D.B. Kerwin, R.G. Leisure, G.R. Eaton, S.S. Eaton, *J. Appl. Phys.* 77 (1995) 790–794.
- [40] J. Weil, *NATO Science Series, II, Mathematics, Chemistry, and Physics, Defects in SiO₂ and Related Dielectrics*, 2000, pp. 197–212.
- [41] G.M. Zhidomirov, K.M. Salikhov, *Sov. Phys. JETP* 29 (1969) 1037–1040.
- [42] M. Brustolon, T. Cassol, L. Micheletti, U. Segre, *Mol. Phys.* 57 (1986) 1005–1014.
- [43] B. Rakvin, N. Maltar-Strmecki, P. Cevc, D. Arcon, *J. Magn. Reson.* 152 (2001) 149–155.
- [44] R. Angelone, C. Forte, C. Pinzino, *J. Magn. Reson.* 101 (1993) 16–22.
- [45] S.A. Dzuba, K.M. Salikhov, Yu.D. Tsvetkov, *Chem. Phys. Lett.* 79 (1981) 568–572.
- [46] I. Miyagawa, K. Itoh, *J. Chem. Phys.* 36 (1962) 2157–2163.
- [47] L. Kispert, M.K. Bowman, J. Norris, I.M. Brown, *J. Chem. Phys.* 76 (1982) 26–30.
- [48] M. Brustolon, T. Cassol, L. Micheletti, U. Segre, *Mol. Phys.* 57 (1986) 1005–1014.
- [49] P.A. Beckmann, C.I. Ratcliffe, B.A. Dunell, *J. Magn. Reson.* 32 (1978) 391–402.
- [50] P.A. Beckmann, F.A. Fusco, A.E. O'Neill, *J. Magn. Reson.* 59 (1984) 63–70.
- [51] J.H. Ardenkjaer-Larsen, I. Laursen, I. Leunbach, G. Ehnholm, L.-G. Wistrand, J.S. Petersson, K. Golman, *J. Magn. Reson.* 133 (1998) 1–12.
- [52] G.E. Santyr, R.M. Henkelman, M.J. Bronskill, *J. Magn. Reson.* 79 (1988) 28–44.
- [53] F. Bloch, *Phys. Rev.* 70 (1946) 460–485.
- [54] N. Bloembergen, E.M. Purcell, R.V. Pound, *Phys. Rev.* 73 (1948) 679–712.
- [55] A. Abragam, *The Principles of Nuclear Magnetism*, Oxford University Press, Oxford, 1961, p. 126 (Chapter 4).
- [56] B. Cowan, *Nuclear Magnetic Resonance and Relaxation*, Cambridge University Press, Cambridge, 1997, pp. 175–177.
- [57] B.C. Gerstein, C.R. Dybowski, *Transient Techniques in NMR of Solids*, Academic Press, Orlando, 1985, pp. 94–103.